

Magnetic and electronic transport properties of the novel compounds  $U_2Co_6Al_{19}$  and  $Th_2Co_6Al_{19}$

This article has been downloaded from IOPscience. Please scroll down to see the full text article.

2004 J. Phys.: Condens. Matter 16 3097

(<http://iopscience.iop.org/0953-8984/16/18/011>)

View [the table of contents for this issue](#), or go to the [journal homepage](#) for more

Download details:

IP Address: 129.252.86.83

The article was downloaded on 27/05/2010 at 14:34

Please note that [terms and conditions apply](#).

# Magnetic and electronic transport properties of the novel compounds $\text{U}_2\text{Co}_6\text{Al}_{19}$ and $\text{Th}_2\text{Co}_6\text{Al}_{19}$

R Troć<sup>1,3</sup>, H Noël<sup>2</sup>, O Tougait<sup>2</sup> and K Wochowski<sup>1</sup>

<sup>1</sup> W Trzebiatowski Institute of Low Temperature and Structure Research, 90-950 Wrocław, PO Box 1410, Poland

<sup>2</sup> Laboratoire de Chimie du Solide et Inorganique Moléculaire, UMR 6511 CNRS–Université de Rennes 1, Avenue du Général Leclerc, 35042 Rennes, France

E-mail: troc@int.pan.wroc.pl

Received 30 December 2003

Published 23 April 2004

Online at [stacks.iop.org/JPhysCM/16/3097](http://stacks.iop.org/JPhysCM/16/3097)

DOI: 10.1088/0953-8984/16/18/011

## Abstract

Experimental results on AC susceptibility, DC magnetization, electrical resistivity and magnetoresistivity up to 8 T have been obtained for a well annealed polycrystalline sample of the novel ternary aluminide  $\text{U}_2\text{Co}_6\text{Al}_{19}$ . As a reference, similar experiments on the Th counterpart were also done. The U-containing aluminide exhibits two phase transitions at 8 and 12.5 K, probably of ferromagnetic and antiferromagnetic type, respectively. Moreover,  $\text{U}_2\text{Co}_6\text{Al}_{19}$  is a Kondo system showing the coherence effect below about 40 K. On the other hand, the Th counterpart showed unexpectedly a spin fluctuation behaviour, which was inferred from the broad maximum seen in its  $\chi(T)$  dependence near 600 K. However, the low temperature variation of  $\rho(T)$  leads rather to an  $AT^{5/2}$  power dependence instead of to the  $AT^2$  one characteristic for a spin fluctuation behaviour.

## 1. Introduction

Among the five uranium heavy fermion superconductors known so far, two of them are ternary aluminides, namely  $\text{UNi}_2\text{Al}_3$  and  $\text{UPd}_2\text{Al}_3$  [1]. We have extended our search for similar phases by recent studies of the U–Co–Al system [2]. We have revealed the existence of as many as four new ternary phases,  $\text{UCoAl}_4$ ,  $\text{U}_2\text{Co}_3\text{Al}_9$ ,  $\text{U}_3\text{Co}_{4+x}\text{Al}_{12-x}$  and  $\text{U}_2\text{Co}_6\text{Al}_{19}$ , which enlarges the series of ternary aluminides. We have already established their crystal structures and we have started an investigation of their fundamental magnetic and electronic transport properties. In this paper, first we will present such data for  $\text{U}_2\text{Co}_6\text{Al}_{19}$  and  $\text{Th}_2\text{Co}_6\text{Al}_{19}$ .

These compounds crystallize in a new type of crystal structure, with four formula units, in the monoclinic space group  $C2/m$ . It can be regarded as a superstructure of  $\text{NdCo}_{4-x}\text{Ga}_9$

<sup>3</sup> Author to whom any correspondence should be addressed.

structure type [3], but with fully ordered positions of atoms. The superstructure results from an ordering of the Al atoms. The same type of structure has been found not only for the Th counterpart [3], but also for the Ce [4] and the remaining rare-earth counterparts [5]. In this structure the shortest U–U distances are found along the *c* direction with alternating values of 3.98 and 4.22 Å, which reflect an eventual localized character of the 5f electrons in this compound. A comparison of the other interatomic distances with the sum of the atomic radii reveals that most of the Al–Al distances and the Co–Al distances in this new structure are shorter, which indicates their dominant covalent character, while those of U–Co and U–Al ones are longer than their respective sums. The latter leads to rather weak bonding interactions between the uranium atoms and their near neighbours. The coordination sphere of the uranium atoms consists of thirteen Al atoms and one Co atom. There, eight Al atoms form a strongly distorted rectangular prism and the remaining five Al atoms are on the corners of an equatorial regular pentagon. There is no direct contact between the central U atom and the surrounding uranium atoms.

## 2. Experimental details

### 2.1. Synthesis and characterization

Polycrystalline samples containing stoichiometric amounts of the high purity constituent elements were prepared by melting in an arc furnace under a purified argon atmosphere. The purity of the starting materials was: 3N for U, 3N for Th, 4N for Co and 5N for Al. The buttons obtained were flipped and remelted three times to achieve homogeneity. The weight losses were less than 1 wt%. For a better homogeneity the samples were annealed in an evacuated quartz tube at 1050 °C for 500 h; this was followed by rapid cooling to room temperature. The powder x-ray diffraction analyses confirmed that the Th- and U-based title compounds were single phases. The lattice parameters were  $a = 17.478(5)$ ,  $b = 12.054(5)$ ,  $c = 8.239(4)$  Å and  $\beta = 103.84(5)^\circ$  for the uranium-containing compound and  $a = 17.517(7)$ ,  $b = 12.143(4)$ ,  $c = 8.262(4)$  Å and  $\beta = 103.56(5)^\circ$  for the thorium-containing compound. The values found for  $\text{U}_2\text{Co}_6\text{Al}_{19}$  are close to those determined from the single-crystal refinement. Metallographic and quantitative analyses (EDX) were made as described previously [3].

Magnetic measurements were carried out in the temperature range 1.9–400 K in the case of U-containing ternaries and 1.9–800 K for Th-containing ternaries using a MPMS Quantum Design SQUID magnetometer. AC susceptibility measurements were performed at 4.2–30 K using an Oxford Instruments susceptometer at frequency 1000 Hz and an amplitude of the AC field of 1 Oe.

Bar shaped specimens of typical dimensions  $1 \times 1 \times 6 \text{ mm}^3$  were cut from Th- and U-containing ingots for electrical resistivity measurements using a standard four-terminal method. The measurements of the magnetoresistivity were made in magnetic fields from zero up to 8 T at temperatures between 4.2 and 45 K.

## 3. Results and discussion

### 3.1. Magnetic properties

Some preliminary studies of magnetic properties of the U-based compound have already been published [3]. At present we compare in figure 1 the DC magnetization taken at 0.5 T (upper panel) and the AC susceptibility data (lower panel) both covering the range of temperatures 1.9–28 K. In this low temperature region the two phase transitions are signalled by both types

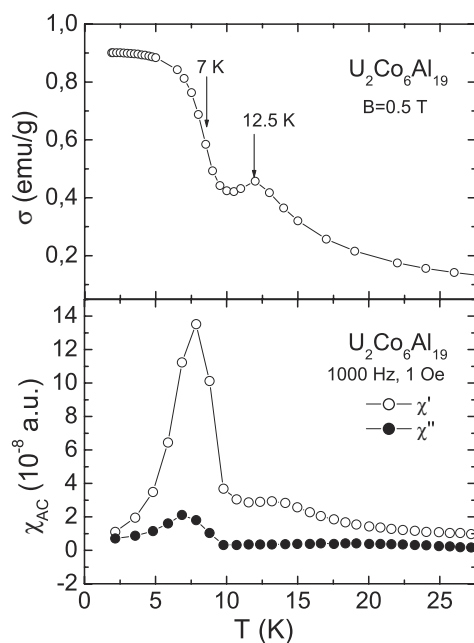


**Figure 1.** Magnetization (upper panel) and AC susceptibility (lower panel) as a function of temperature for  $U_2Co_6Al_{19}$ .

of measurements. The first transition denoted as  $T_C$  occurs at 8 K as an inflection point on the  $\sigma(T)$  curve or as a strong peak in the real part of AC susceptibility,  $\chi'(T)$ , at almost the same temperature. Also the out-of-phase component,  $\chi''(T)$ , forms a shoulder around 8 K which, together with the temperature dependence of the in-phase susceptibility  $\chi'(T)$ , reflects the characteristic behaviour of a ferromagnet. However, the magnetization curves versus applied magnetic field up to 5 T, shown in figure 2 at temperatures 1.9, 3.0 and 6.0 K (upper panel), have rather small saturation values and at the lowest temperature measured this amounts to  $0.36 \mu_B/U$  atom, assuming Co to be nonmagnetic. The second transition denoted as  $T_N$ , probably of antiferromagnetic character, occurs as a small peak in both the  $\sigma(T)$  and  $\chi'(T)$  curves at approximately the same temperature of 12.5 K (see figure 1). The magnetization curves taken at 9, 12, 15 and 18 K, which are shown in the lower panel of figure 2, give evidence of metamagnetic character with the critical field as low as 0.3 T. Note the different characters of the magnetization curves taken for the two sets of temperatures given above.

As figure 3 displays, the inverse susceptibility versus temperature dependence is curvilinear with a rapid decrease toward the temperature axis below about 50 K, reminiscent of the ferrimagnetic type of behaviour or/and caused by a strong influence of crystal field interactions. A fit of the magnetic susceptibility to the modified Curie–Weiss law, made in the range of temperatures 60–400 K, yields an effective magnetic moment of uranium  $\mu_{\text{eff}} = 2.5 \mu_B/U$  atom, a paramagnetic Curie temperature  $\theta_p = -34$  K and a term  $\chi_0 = 0.5 \times 10^{-3} \text{ emu mol}^{-1}$  independent of temperature. An approximation of the temperature dependence of the susceptibility by just a Curie–Weiss (CW) law at temperatures above 200 K leads to  $\mu_{\text{eff}} = 3.0 \mu_B/U$  atom and  $\theta_{CW} = -94$  K, which seem to be more adequate magnetic parameters than those inferred from the modified CW law. These values are then associated with a more highly localized system of 5f magnetic moments with which we are probably concerned in  $U_2Co_6Al_{19}$ . Usually the curvilinear character of the inverse susceptibility

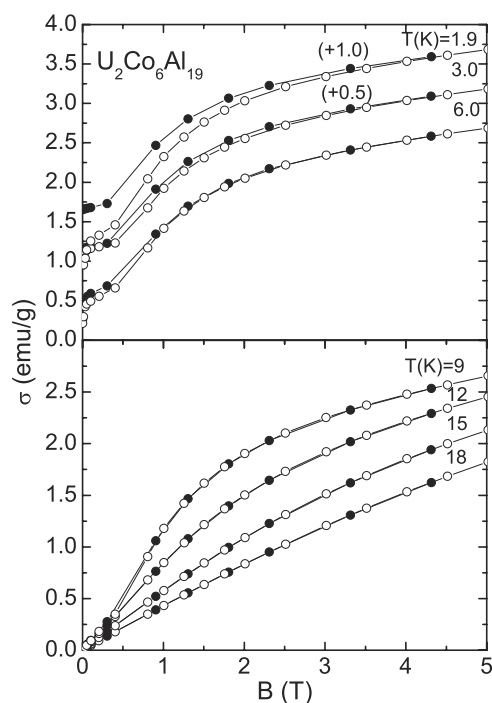


**Figure 2.** Magnetization as a function of applied magnetic field taken at different temperatures from 1.9 to 18 K for  $\text{U}_2\text{Co}_6\text{Al}_{19}$ .

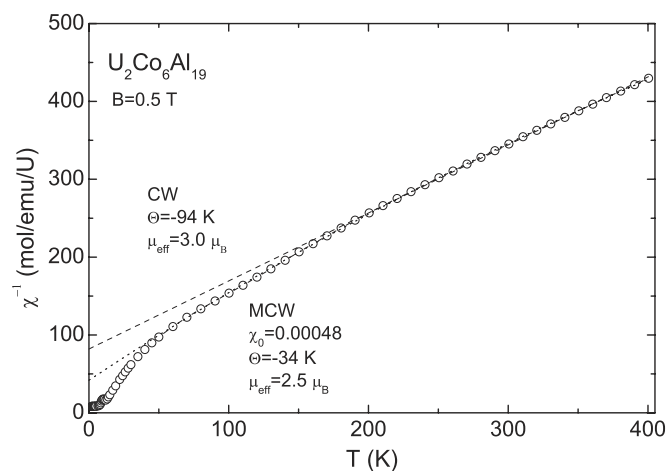


**Figure 3.** The temperature dependence of the inverse susceptibility of  $\text{U}_2\text{Co}_6\text{Al}_{19}$ .

found for polycrystalline materials is a result of averaging at least three different temperature dependences of the susceptibility due the low symmetry of the unit cell of  $\text{U}_2\text{Co}_6\text{Al}_{19}$ . The relatively large  $\theta_{\text{CW}}$  absolute value may also refer to Kondo-type interactions, if we are neglecting crystal field splitting [6].

The magnetic properties of  $\text{Th}_2\text{Co}_6\text{Al}_{19}$  are displayed in figure 4 in the form of the susceptibility as a function of temperature measured up to 800 K. The obtained tendency for

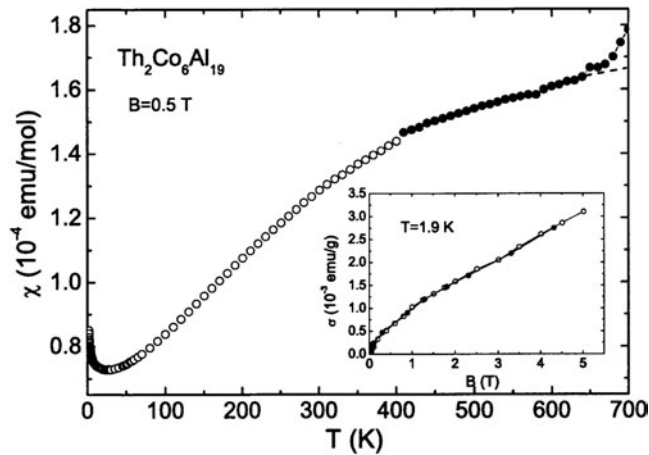


**Figure 4.** Magnetic susceptibility as a function of temperature for  $Th_2Co_6Al_{19}$ . Open and closed points indicate the measurements made in two different ways using the SQUID. Inset: magnetization versus magnetic field measured in increasing (open points) and decreasing (closed points) fields. The hysteresis is negligible.

the susceptibility to reach a maximum at about 600 K gives evidence for a spin fluctuation (SF) character of the Co behaviour in its 3d electron band. This means that cobalt still has some holes in its band after transferring the Th valence electrons to this band, which allows it to carry some itinerant moments. They probably fluctuate in a similar way to those in the well known family of the  $ACo_2$  type of intermetallic compounds, where A is Sc, La or Lu (see a review in [7]). However, a better similarity exists in the comparison to  $ZrCo_2$  and  $HfCo_2$  [8] having higher d electron concentration. Like Th, Zr and Hf also provide two d electrons per formula unit into the corresponding d bands, while the A atoms contribute only one d electron into the conduction bands. As a result of this difference the  $\rho(T)$  curvature of higher d electron density compounds is much less pronounced compared to that of  $ACo_2$  compounds. This implies that the spin fluctuation temperatures are considerably higher than those of the  $ACo_2$  group. A necessary prerequisite for the appearance of SF in a given material is an enhanced value of the electron density of states close to the Fermi level ( $E_F$ ) together with its steep negative slope and a positive curvature near  $E_F$ . The temperature of the maximum in  $\chi(T)$  is often regarded as that of a crossover to a regime with a constant SF amplitude independent of temperature. Above  $T_{max}$  a CW behaviour of  $\chi(T)$  may be expected. However, carrying out the measurements only in a limited range of temperatures up to 800 K, it was not possible to check this prediction.

### 3.2. Electronic transport properties

Evidence of two phase transitions in  $U_2Co_6Al_{19}$  is found also from resistivity measurements,  $\rho(T)$ , as displayed in the inset of figure 5, where the temperature derivative of the electrical resistivity is presented. One can see that the characters of these two transitions are different. Whereas at the lower temperature phase transition at  $T_C$  this derivative goes through a sharp peak, that at higher temperature, at  $T_N$ , is presented as a shoulder of  $\lambda$  type. In general, the resistivity increases with decreasing temperature (see figure 5) in the Kondo-like manner down to the vicinity of 50 K, where  $\rho(T)$  goes through a pronounced maximum. Below this temperature,  $\rho(T)$  goes through a very broad knee and then in the vicinity of 40 K it drops rapidly almost to a quarter of its value to achieve finally a residual value,  $\rho_0$ , of  $125 \mu\Omega$  cm.

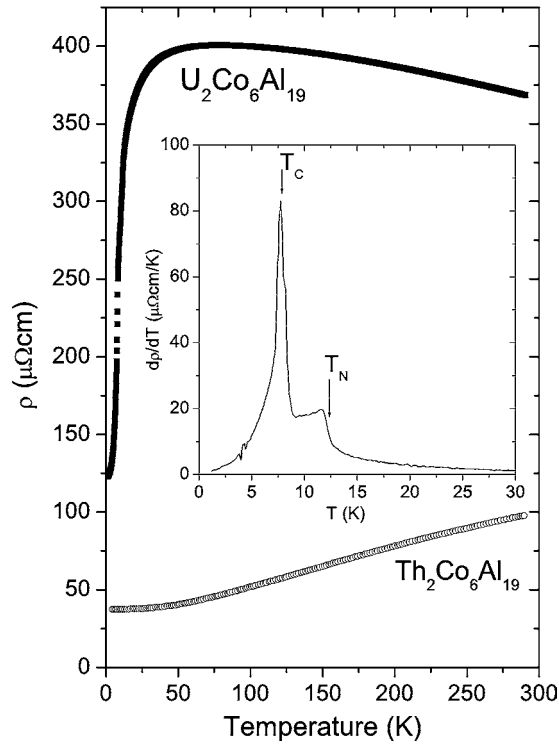


**Figure 5.** Electrical resistivity for  $\text{Th}_2\text{Co}_6\text{Al}_{19}$  and  $\text{U}_2\text{Co}_6\text{Al}_{19}$  as a function of temperature. Inset: the temperature derivative of the electrical resistivity for  $\text{U}_2\text{Co}_6\text{Al}_{19}$  at low temperatures.

This effect is probably caused by the occurrence of the coherence in electron scattering at  $T_{\text{coh}} \sim 40$  K.

The electrical resistivity data for the reference compound  $\text{Th}_2\text{Co}_6\text{Al}_{19}$  are displayed in figure 6. This behaviour is of typical metallic character, with the characteristic ‘hockey stick’ shape of the  $\rho(T)$  dependence. The solid line superimposed onto the data of figure 6 gives evidence of a reasonably good LSQ fit to the Grüneisen–Bloch electron–phonon scattering relation [9]:

$$\rho = \rho_0 + 4R\theta_R \left(\frac{T}{\theta_R}\right)^5 \int_0^{\theta_R/T} \frac{x^5 dx}{(e^x - 1)(1 - e^{-x})} + KT^3$$

where  $\rho_0 = 38 \mu\Omega \text{ cm}$ ,  $R$  is a constant and  $\theta_R = 320$  K is the characteristic resistivity Debye temperature. The cubic term  $KT^3$  describes the interband scattering process [10] ( $K = 1.8 \times 10^{-7} \mu\Omega \text{ cm K}^{-3}$ ). On the other hand, we present in the inset of figure 6 the low temperature  $\rho(T)$  as a power dependence on  $T^{5/2}$ , which holds up to 75 K. The power exponent obtained,  $n = 5/2$ , is in disagreement with the spin fluctuation relation:  $\rho_{\text{SF}} = AT^2$ , predicted by theory [7]. Also, the required tendency of the resistivity to saturation at elevated temperatures is not distinctly apparent.

By subtracting from the total measured resistivity the temperature-dependent part of  $\rho(T)$  for the non-f electron reference Th compound, together with the respective residual resistivity,  $\rho_0$ , we were able to obtain the 5f electron part of the resistivity,  $\rho_{5f}$ , only. The resulting difference describing the  $\rho_{5f}(T)$  curve, but with added  $\rho_0$ , is shown in figure 7 on a semilogarithmic scale. In addition, the results for  $\text{Th}_2\text{Co}_6\text{Al}_{19}$  are also presented for

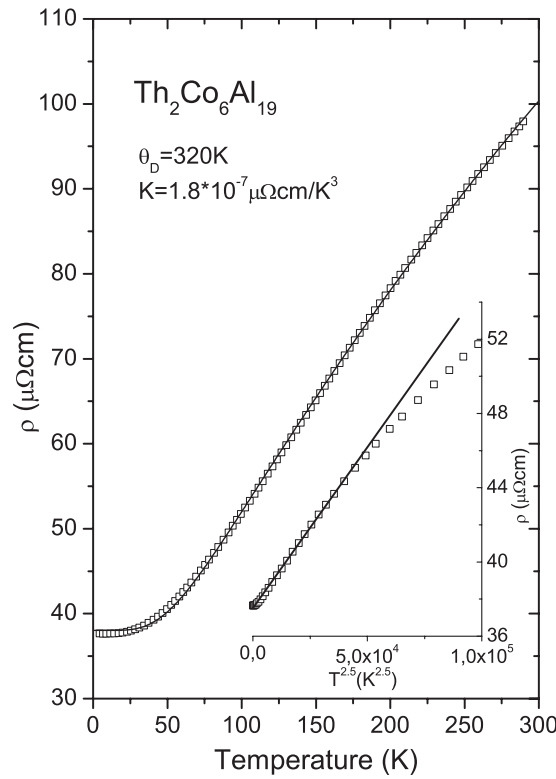


**Figure 6.** Electrical resistivity of  $Th_2Co_6Al_{19}$  as a function of temperature with the fitting to the Grüneisen–Bloch equation. Inset: the fitting to the  $AT^{5/2}$  power dependence.

comparison with the low temperature power variation  $T^{2.5}$  marked as a solid curve. In many uranium-based, nearly local moment systems, such a distinct increase in the electrical resistivity with decreasing temperature as the logarithmic dependence:  $\rho_{5f}(T) = c_K \ln(T/T_K)$ , is associated with an incoherent Kondo scattering of conduction electrons of the f electron moment ( $T_K$  is the Kondo temperature). This relation is valid here above 200 K and is presented in figure 7 by means of an LSQ fit to the  $\rho_{5f}(T)$  data, also shown as a solid curve. However, it is rather too short a temperature range of fitting for attributing any meaning to the fitting parameters given in the figure. The maximum around 50 K may indicate the overall crystal field splitting of the  $U^{4+}(5f^2)$  ion ground term,  ${}^3H_4$ , concurring with the Kondo interactions. We ascribe then the observed drop in  $\rho(T)$  below 40 K to the formation of a Kondo lattice. It is interesting to note that this feature is found at a temperature much higher than the low temperature phase transitions to the ordered states, clearly seen in this figure in the form of knees at  $T_C$  ( $=8$  K) and  $T_N$  ( $=12.5$  K). These phase transition temperatures agree well with those inferred from the magnetic data as shown in figure 1. The low temperature behaviour of  $\rho(T)$ , between 0.3 and 8 K, can be fitted to an energy gap variation [10], the formula of which together with the Fermi liquid term  $AT^2$  is given in figure 7. In this figure the low temperature  $\rho(T)$  curve determined in an applied magnetic field of 8 T is also plotted. As a result of the LSQ fit, a pure  $T^2$  dependence up to 12 K has been found which means that the energy gap established in zero field as 37 K has been cancelled by applying the magnetic field. In such a situation, both the spin waves and Fermi



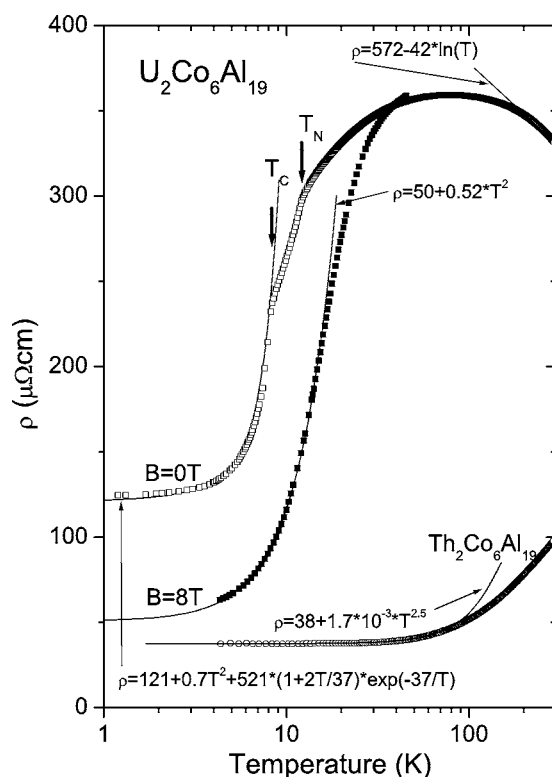


**Figure 7.** A semilogarithmic plot of  $\rho$  versus  $T$  taken in zero and an 8 T magnetic field for  $\text{U}_2\text{Co}_6\text{Al}_{19}$  and a similar zero-field plot of  $\rho$  versus  $T$  for  $\text{Th}_2\text{Co}_6\text{Al}_{19}$ . Note that the 8 T curve has been shifted down by  $30 \mu\Omega \text{ cm}$ .

liquid dependences have the same  $T^2$  variation. As we will see below, under the applied magnetic fields at temperatures above  $T_C$  a metamagnetic transition occurs instead of zero-field antiferromagnetism.

Finally, figure 8 displays the field (left-hand panel) and temperature (right-hand panel) dependences of the magnetoresistivity (MR) of  $\text{U}_2\text{Co}_6\text{Al}_{19}$ , defined as  $\Delta\rho/\rho = [\rho(B) - \rho(0)]/\rho(0)$ . This quantity results in a giant negative value amounting in this compound even to 60% at 4.2 K. The  $\Delta\rho/\rho$  curve taken at this temperature and 5 K is shaped in weak fields as that of the magnetization curve reversed in sign, exhibiting some hysteresis, but also with some competing behaviour in higher magnetic fields, leading to a broad maximum in  $\Delta\rho/\rho(B)$  at about 4 T. The latter feature signals the existence of another component in MR, probably with positive sign, which at present we leave for more detailed studies planned on a single crystal. Then, the curve taken at 10 K represents a typical metamagnetic behaviour expected in the case of an antiferromagnetic aligning of the magnetic moments in zero field. Such a jump in MR is a common feature in Kondo lattice materials in both the Ce [11] and U intermetallics [12]. However, no distinct hysteresis is, this time, observed, like in the curve measured at 15 K, but yielding at 8 T in the latter case a much lower MR value of 38%. The character of the  $\Delta\rho/\rho$  versus  $B$  dependences changes from concave to convex, which is seen very distinctly in isotherms at temperatures higher than 15 K, for which the absolute MR values fall in the way illustrated by the MR variation at 20 K. Thus, such a behaviour with a convex field dependence is reminiscent of a Kondo-like interaction. However, the MR values taken above 20 K are very

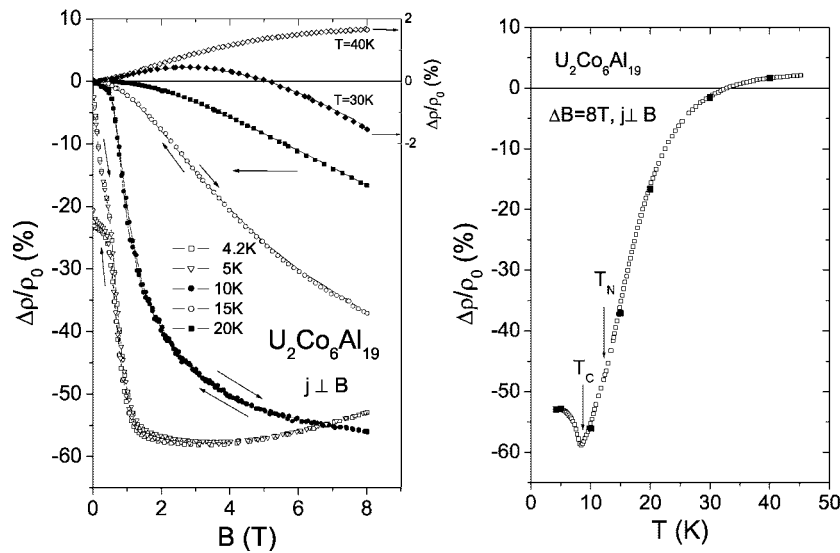


**Figure 8.** Magnetoresistivity MR of  $U_2Co_6Al_{19}$  as a function of applied magnetic field (left-hand panel) and of temperature (right-hand panel).

small (see the right-hand scale) and MR already becomes slightly positive at 30 K up to a field of 5 T, where it changes its sign to negative. MR becomes completely positive up to 8 T at 40 K. We suppose that the positive MR is due to the cyclotron motion of the carriers with enhanced masses and also due to the predominance at these temperatures of the coherence effect, which as a rule leads to positive MR. The isofield temperature variation of MR taken at 8 T is presented in figure 8 (right-hand panel). It illustrates the rapid increase of this absolute quantity with decreasing temperature. Note that this curve simultaneously follows the experimental points (solid squares) found from the isothermal  $\Delta\rho/\rho(B)$  curves at 8 T. Moreover, this isofield  $\Delta\rho/\rho(T)$  variation shows only a small change in slope at the temperature close to  $T_N$  and a distinct sharp minimum at  $T_C$ , both temperatures found at zero field. It is readily noticeable in figure 8 (right-hand panel) that at temperatures below  $T_{coh} \sim 40$  K there is a rapid growth in the absolute MR up to a giant value of about 60% just at the zero-field  $T_C$  ( $=8$  K). As we have already mentioned above and also illustrated in figure 7, the power exponent in the low temperature variation,  $\rho(T) \sim T^n$ , changes from  $n = 5/2$  in the zero-field regime into a Fermi liquid one with  $n = 2$  at 8 T.

#### 4. Concluding remarks

By analogy to the similar overall behaviour of  $\rho(T)$ , reported previously for all heavy fermion uranium-containing superconductors known to date, we could also expect a superconducting behaviour for  $U_2Co_6Al_{19}$ . However, the low temperature tendency of its  $\rho(T)$  of reaching saturation, as evidenced by measurements carried out down to 0.3 K (see figure 7), has not revealed such properties.

Apart from the absolute  $\rho$  values, the temperature dependence of the resistivity of  $UPd_2Al_3$  is quite similar to that illustrated in figure 5, with the exception that it shows a clear maximum at a higher temperature of around 80 K. This similarity comprises a pronounced decrease of  $\rho$  toward lower temperatures and a kink at the transition into an antiferromagnetic state around 14 K [1c]. Also its temperature derivative of the resistivity at  $T_N$  is manifested by

an anomaly, of  $\lambda$  type, similar to that of  $\text{U}_2\text{Co}_6\text{Al}_{19}$ , as shown in figure 5. However, the low temperature field dependence of the magnetoresistivity is distinctly different [11]. Below  $T_N$  and in fields up to 7 T, MR is positive and exhibits a saturation to rather small  $\Delta\rho/\rho$  values of 1–2% at temperatures above 3 K. The difference in sign and magnitude with respect to  $\text{U}_2\text{Co}_6\text{Al}_{19}$  is quite well explained, because  $\text{UPd}_2\text{Al}_3$  has its metamagnetic transition at a magnetic field as high as 18 T [13]. Like  $\text{U}_2\text{Co}_6\text{Al}_{19}$ , this superconducting aluminide exhibits a precipitous negative drop of about 50% in the transverse MR ( $j \parallel c$ ,  $B \parallel b$ ) at 4.2 K in a critical field of 18 T [12]. It seems that the observed difference, for example between the two compounds  $\text{U}_2\text{Co}_6\text{Al}_{19}$  and  $\text{UPd}_2\text{Al}_3$  [1b, 1c], arises because the former compound goes, below 8 K, into the ferromagnetic state, whereas the latter one retains, over all temperatures below  $T_N$  (=14.2 K), its antiferromagnetic state. Thus it seems that this is the main reason for not observing superconductivity in the case of the novel ternary uranium aluminide  $\text{U}_2\text{Co}_6\text{Al}_{19}$ , while  $\text{UPd}_2\text{Al}_3$  is a superconductor below 2 K [1b]. It is noteworthy that the moderately heavy fermion, antiferromagnetic  $\text{UPd}_2\text{Ga}_3$  ( $T_N = 13$  K), crystallizing in a hexagonal superstructure of the  $\text{PrNi}_2\text{Al}_3$  type, is not a superconductor down to 50 mK [13], despite showing behaviour of  $\rho(T)$  similar to that of the two compounds mentioned above. No key reason for the absence of superconductivity in this gallide has been given in [14].

### Acknowledgments

The work was supported partially by the exchange programme of the Polish Academy of Sciences and CNRS, under project 6386.

The authors thank Dr A Zaleski for carrying out the AC susceptibility measurements, Dr R Wawryk for making the low temperature electrical resistivity measurements and Mrs D Badurski and R Gorzelniak for their assistance in transport and magnetic measurements.

### References

- [1a] Geibel C, Thies S, Kaczorowski D, Mehner A, Granel A, Seidel B, Ahlheim U, Helfrich R, Petersen K, Bredl C D and Steglich F 1991 *Z. Phys. B* **83** 305
- [1b] Geibel C, Schanke C, Thies S, Kitazawa H, Bredl C D, Böhm A, Rau M, Granel A, Caspary R, Helfrich R, Ahlheim U, Weber G and Steglich F 1994 *Z. Phys. B* **84** 1
- [1c] Haga Y, Yamamoto E, Inado Y, Aoki D, Tenya K, Ikeda M, Sakakiba T and Onuki Y 1996 *J. Phys. Soc. Japan* **65** 3646
- [2] Noël H *et al* 2004 to be published
- [3] Tougait O, Stępień-Damm J, Zaremba V, Noël H and Troć R 2003 *J. Solid State Chem.* **174** 152
- [4] Kaczorowski D, Tougait O, Czopnik A, Marucha Cz and Noël H 2004 *J. Magn. Magn. Mater.* at press
- [5] Tougait O *et al* 2004 to be published
- [6] Hawson A 1993 *The Kondo Problem to Heavy Fermions* (Cambridge: Cambridge University Press)
- [7] Gratz E and Markosyan A S 2001 *J. Phys.: Condens. Matter* **13** R385
- [8] Baranov N, Bauer E, Gratz E, Hauser R, Markosyan A and Resel R 1993 *Proc. Int. Conf. on Physics of Transition Metals* vol 1, ed P M Oppener and J Kübler (Singapore: World Scientific) p 370
- [9] Meaden G H 1965 *Electrical Resistance of Metals* (New York: Plenum)
- [10] Andersen N H and Smith H 1979 *Phys. Rev. B* **19** 384
- [11] See for example, Onuki Y, Nakei Y, Omi T, Yamazaki T and Komatsubara T 1988 *J. Magn. Magn. Mater.* **76/77** 119
- [12] Köhler R, Diehl J, Fischer H, Sato N, Komatsubara T, Geibel C and Steglich F 1993 *Physica B* **186–188** 288
- [13] Visser A De, Bakker K, Tai L T, Menovsky A A, Mentiuk S A M, Wienwenhuys G J and Mydosh J A 1993 *Physica B* **168–188** 297
- [14] Süllow S, Ludoph B, Becker A, Nieuwenhuys G J, Menovsky A A and Mydosh J A 1995 *Phys. Rev. B* **52** 12784